Original

Sonographic findings of malignant peripheral nerve sheath tumors – case series –

Maiko Osaka[*1], †Tomonori Kishino,*[*1,2,3], Naoko Shimamori*[*1], Satsuki Matsushima*[*2], Satoko Yamasaki*[*1,2], Kouki Ohtsuka*[*1,2], Hiroki Yasudo*[*1,2], Takeshi Morii*[*4], Junji Shibahara*[*5], Takashi Watanabe*[*6], Hiroaki Ohnishi*[*1,2]

†Correspondence: Kyorin University Faculty of Health Sciences, 5-4-1 Shimorenjaku, Mitaka, Tokyo 181-8612, Japan
E-mail: kishino@ks.kyorin-u.ac.jp
Received April 28, 2023; accepted June 8, 2024
*1 Department of Clinical Laboratory, Kyorin University Hospital, Tokyo, Japan
*2 Department of Laboratory Medicine, Kyorin University School of Medicine, Tokyo, Japan
*3 Department of Clinical Engineering, Kyorin University Faculty of Health Sciences, Tokyo, Japan
*4 Department of Orthopaedic Surgery, Kyorin University School of Medicine, Tokyo, Japan
*5 Department of Pathology, Kyorin University School of Medicine, Tokyo, Japan
*6 President, Kyorin University, Tokyo, Japan

ABSTRACT

Purpose: Malignant peripheral nerve sheath tumor (MPNST) is a sarcoma deriving from peripheral nerves, accounting for 3–10% of all malignant soft tissue tumors. Around half of cases develop secondary to neurofibromatosis type 1 (NF1). While magnetic resonance imaging has been considered the best imaging modality for diagnosing MPNST, the efficacy of sonography has not been precisely investigated. The present study therefore aimed to clarify the sonographic findings for this rare entity in a case series.
Methods: Sonographic findings of four cases with MPNST that had been diagnosed by histopathological studies of specimens obtained via biopsy or surgical resection in our hospital between 2013 and 2023 were evaluated. Age range was 51–56 years and three of the four patients were male. MPNST developed secondary to NF1 in three cases, and the tumors had developed in the thigh and retroperitoneum in two cases each. All cases showed rapid tumor growth within 1 year.
Results: The MPNSTs were large masses appearing hypervascular on Doppler images. Although shapes and contours varied, MPNSTs were depicted as heterogeneously hypoechoic masses with well-defined margins. The well-defined margin is distinct from findings observed in most malignant soft-tissue tumors.
Conclusion: Development of MPNST should be considered when a well-defined margin is observed on sonography of rapidly growing masses in soft tissues, particularly in patients with NF1. 〔Lab Med Int 2024; 3(3): 74-83〕

Key Words
malignant peripheral nerve sheath tumor (MPNST), soft-tissue tumor, sonography, well-defined margin

I. Introduction

Malignant peripheral nerve sheath tumor (MPNST) is a sarcoma deriving from peripheral nerves, accounting for 3–10% of all malignant soft-tissue tumors[1)-3)]. Around 50% of MPNSTs occur as transformation from neurofibroma in patients with neurofibromatosis type 1 (NF1), also known as von Recklinghausen's disease, an autosomal dominant disorder[4) 5)]. Conversely, around 5–15% of patients with NF1 develop MPNST. About 10% of MPNSTs arise in the setting of prior radiation therapy, and the remaining up to 50% of MPNST arise de novo from the peripheral nerve sheath[6)]. Common sites of development are the extremities and trunk, followed by the head and neck, with poor prognosis due to the high malignancy in terms of local recurrence and hematogenous metastasis.

Imaging examinations are therefore essential for differentiation from benign tumors and other soft-tissue malignancies. Magnetic resonance imaging (MRI) in combination with ^{18}F-fluorodeoxyglucose positron emission tomography (PET) has been a gold standard imaging modality to distinguish MPNST from benign peripheral nerve sheath tumors (PNSTs) such as neurofibroma [1)7)8)]. Meanwhile, sonography has been utilized as an initial imaging modality for screening examinations, taking advantage of its ready accessibility, non-invasiveness and inexpensiveness. We have reported that malignant soft tissue tumors generally appear as a large mass with ill-defined margins and hypervascularity on sonography [9)]. However, the appearance of the MPNST margin on imaging has reportedly varied among studies. A cohort study utilizing sonography found that MPNST presented with an ill-defined margin [10)]. In contrast, MPNST exhibits well-defined or partially ill-defined margins on MRI when compared with non-neurogenic malignant soft tissue tumors [11)]. The present study therefore aimed to clarify the features of MPNST on sonography using findings from a case series.

II. MATERIALS AND METHODS

Institutional case series

MPNST cases pathologically diagnosed in our hospital from October 2013 to December 2023 were included in the present study. Only cases in which sonographic examinations had been performed before surgery or biopsy were included. Cases in which chemotherapy and/or radiation therapy were performed before imaging examinations were excluded. In this period, four cases with MPNST meeting these requirements were identified. This study was approved by the ethics committee at our institute (approval no. 1956) and performed in accordance with the ethical standards formulated in the Declaration of Helsinki and its revisions. The aim, significance, and protocol of the study were disclosed on the website of our hospital and made available to the public (https://www.kyorin-u.ac.jp/hospital/clinic/support02/pdf/support02_optout202209.pdf). Patients were assured of the right to opt out of the use of their data at any time if they declared to the institution their decision not to be integrated into the study. All study procedures met the requirements of the Ethical Guidelines for Medical and Health Research Involving Human Subjects of the Japanese government.

Sonographic examination

Sonographic examinations were performed using an Aplio500 ultrasound system (Canon Medical Systems Corporation, Tochigi, Japan), with the combination of a 3.5-MHz convex-array transducer and an 8.0- or 10.0-MHz linear-array transducer. Examinations were performed by one of the sonographers with more than 10 years of experience and specializing in sonographic examination in our hospital. Tumor location, shape, size, margin, echogenicity, and texture were evaluated on gray-scale images, and vascularity was evaluated on images from Doppler sonography [9)12)-14)]. All sonographic findings other than tumor size were evaluated independently on the basis of preserved images in the sonographic machine by two sonographers certified as experts on soft-tissue sonography by The Japan Society of Ultrasonics in Medicine. Both sonographers were blinded to histology, then a consensus was reached [9)13)14)].

III. RESULTS

Case 1

A 51-year-old man had been diagnosed with NF1 based on the development of multiple neurofibromas on his body at another clinic. He complained of rapid growth of a lesion in the left thigh from 3 cm to 20 cm in the last 6 months, accompanied by neurological symptoms of lumbago. Sonographic examination in our hospital revealed a hypoechoic oval mass with a maximum diameter of 210 mm in the muscle layer of the left thigh (**Figure 1a, b**). Although the margin was well-defined and the contour was regular, textures in the tumor were heterogeneous intermingled with anechoic areas. Doppler sonography showed moderate vascularity at the tumor periphery. MRI also showed a relatively well-demarcated mass measuring 200 × 85 × 70 mm across the left rectus femoris and sartorius muscles. The mass exhibited signal hypointensity compared with surrounding muscle on T1-weighted imaging, and heterogeneous signal hyperintensity on T2-weighted imaging (**Figure 2a, b**). Contrast-enhanced MRI demonstrated heterogeneous enhancement at the tumor periphery, but no enhancement at the center of the tumor suggestive of liquid components was observed. Macroscopic examination of the resected tumor revealed a nodular lesion with necrosis and hemorrhage. Microscopically, the lesion showed fascicular growth of atypical spindle tumor cells with alternating hyper- and hypocellular areas (**Figure 3a**). Tumor cells were focally immunoreactive to S-100 and exhibited partial skeletal muscle differentiation [5)]. Mitotic figures were present at a rate of 20–25 per 10 high-power fields. These findings led to a diagnosis of MPNST with skeletal muscle differentiation (malignant triton tumor).

Case 2

A 56-year-old man with no history of NF1 presented with a 10-year history of a mass in the right thigh. The mass had increased in size over the last 6 months, causing right leg pain. Sonographic examination revealed a hypoechoic, lobular mass measuring 97 mm in diameter, with partial hyperechoic areas in the muscle layer of the right thigh (**Figure 1c, d**). Although the margin was well-defined, the internal texture was heterogeneous. Doppler sonography showed hypervascularity mainly in the center of the mass. MRI also showed a mass measuring 90 × 70 × 60 mm in the adductor longus muscle (**Figure 2c, d**). The mass exhibited signal isointensity as compared with surrounding muscle on T1-weighted imaging, and heterogeneous signal hyperintensity on T2-weighted imaging. The mass was biopsied, revealing a lesion comprising fascicular growth of atypical spindle cells (**Figure 3b**). Mitotic figures were present at a rate of 20–25 per 10 high-power fields. On im-

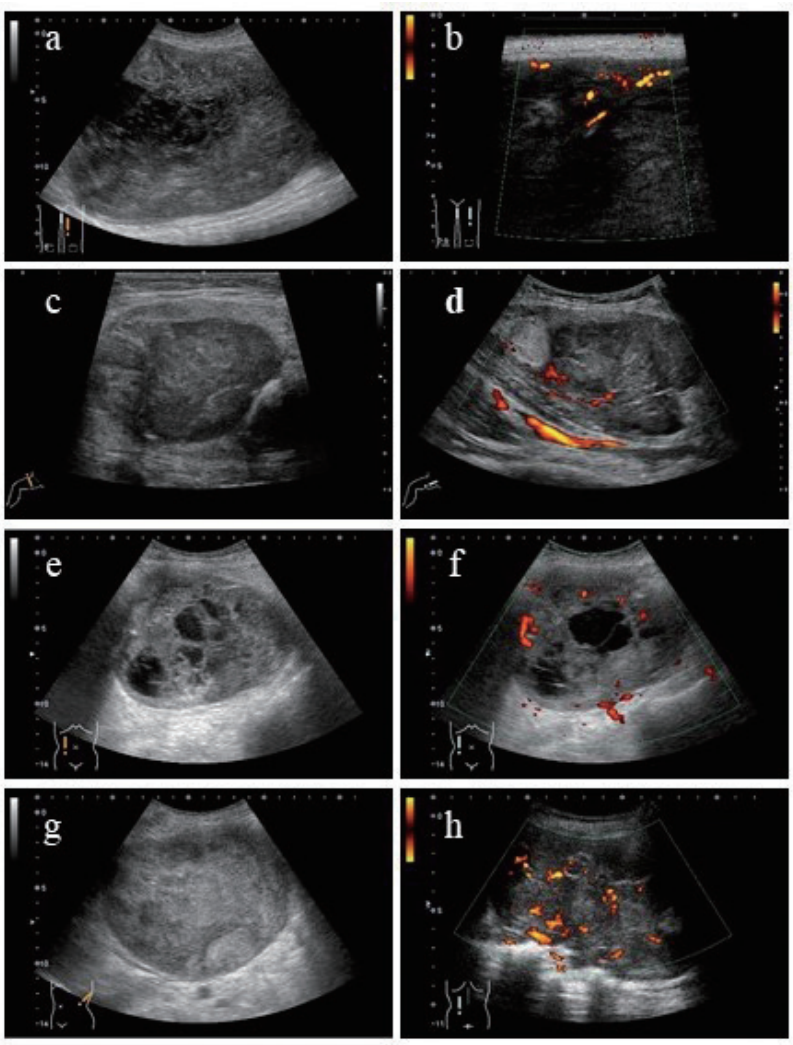

Figure 1

a, b) The tumor presents as an oval mass, 210 mm in maximal diameter on sonography. The mass exhibits heterogeneous hypoechoic intermingled with anechoic areas. The margin is well-defined. Doppler sonography shows moderate vascularity at the tumor periphery.

c, d) The tumor presents as a lobulated mass, 97 mm in size on sonography. The mass appears heterogeneously hypoechoic. The margin of the mass, however, is well-defined. Doppler sonography shows hypervascularity, mainly in the center of the mass.

e, f) The tumor presents as a rounded mass, 119 mm in diameter on sonography. The mass exhibits intermingled heterogeneous hypoechoic and anechoic areas. The margin of the mass is well-defined. Doppler sonography shows hypervascularity with internal vessels.

g, h) The tumor presents as two irregular masses measuring 144 mm and 128 mm on sonography, which thereafter turned out to be one connected lesion. The mass appears heterogeneously hypoechoic. The margin of the mass is, however, well-defined. Doppler sonography shows hypervascularity with internal vessels.

munohistochemistry, the tumor exhibited focal reactivity to S-100 and loss of H3K27me3 [5) 15)]. These findings led to a diagnosis of MPNST.

Case 3

A 56-year-old man had a history of lower limb amputation due to NF1. He recognized a rapidly growing abdominal mass within the preceding year. Sonographic examination at our hospital revealed three hypoechoic, rounded masses with diameters of 119 mm, 60 mm and 48 mm. The rapidly growing mass was considered to correspond to the 119-mm lesion (**Figure 1e, f**). Although the margin was well-defined and the contour was regular, textures in the tumor were intermingled with heterogeneous and anechoic areas. Doppler sonography showed hypervascularity with internal vessels. MRI showed a fusiform mass suggestive of neurogenic tumor in the retroperitoneum,

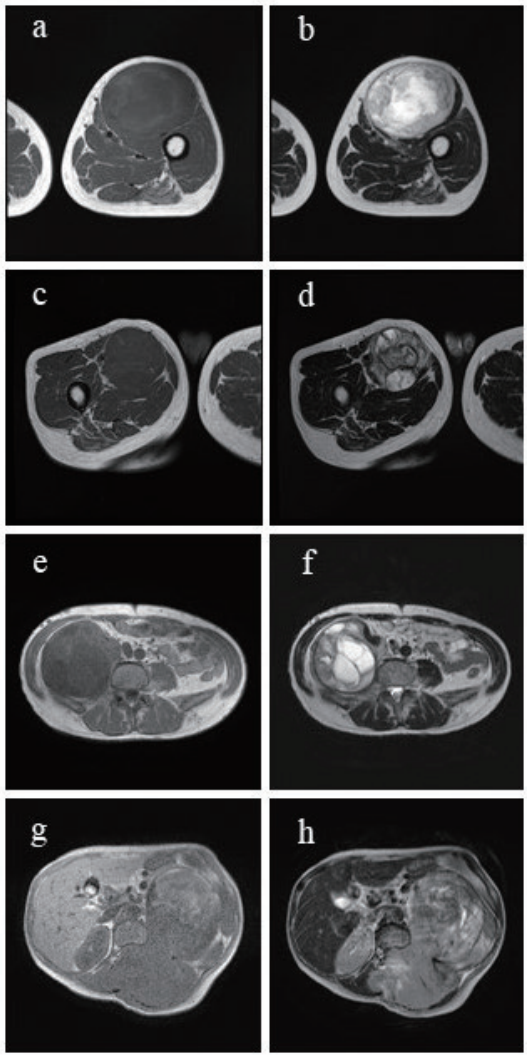

Figure 2

a, b) MRI shows a relatively well-demarcated mass measuring 200 × 85 × 70 mm across the left rectus femoris and sartorius muscles. The mass exhibits signal hypointensity as compared with surrounding muscle on T1-weighted imaging, and heterogeneous signal hyperintensity on T2-weighted imaging.

c, d) MRI shows a mass measuring 90 × 70 × 60 mm in the adductor longus muscle. The mass exhibits signal isointensity as compared with the surrounding muscle on T1-weighted imaging, and heterogeneous signal hyperintensity on T2-weighted imaging.

e, f) MRI shows a fusiform mass suggesting a neurogenic tumor, 115 × 95 × 85 mm, in the retroperitoneum and ventral to the right iliopsoas muscle. The mass exhibits signal hypo- and isointensity as compared with surrounding muscle on T1-weighted imaging, and heterogeneous signal hyperintensity intermingled with signal hypointense septa on T2-weighted imaging.

g, h) MRI shows a mass, 160 × 110 mm, in the left retroperitoneum, including erector spinae muscles. The mass exhibits heterogeneous hypo- to isointensity as compared with abdominal fat or muscle on T1-weighted imaging, and heterogeneous isointensity intermingled by signal hyperintensity on T2-weighted imaging.

measuring 115 × 95 × 85 mm and ventral to the right iliopsoas muscle (**Figure 2e, f**). The mass exhibited signal hypo- to isointensity compared with surrounding muscle on T1-weighted imaging, and heterogeneous signal hyperintensity intermingled with signal hypointense septa on T2-weighted imaging. Contrast-enhanced MRI showed increased enhancement at the tumor periphery in the early phase of enhancement and much more enhancement in the late phase of enhancement. A biopsy specimen obtained from the largest mass revealed mitotic figures at a rate of over 50 per 10 high-power fields and intermingled necrotic regions, leading to a final diagnosis of MPNST composing highly atypical tumor cells (anaplastic MPNST) (**Figure 3c**).

Case 4

A 55-year-old woman with NF1 had been suffering from lumbago for 1 year. A mass was identified from the back to retroperitoneum. Sonographic examination in our hospital revealed two irregular, hypoechoic masses with maximum diameters of 144 mm and 128 mm (**Figure 1g, h**). Al-

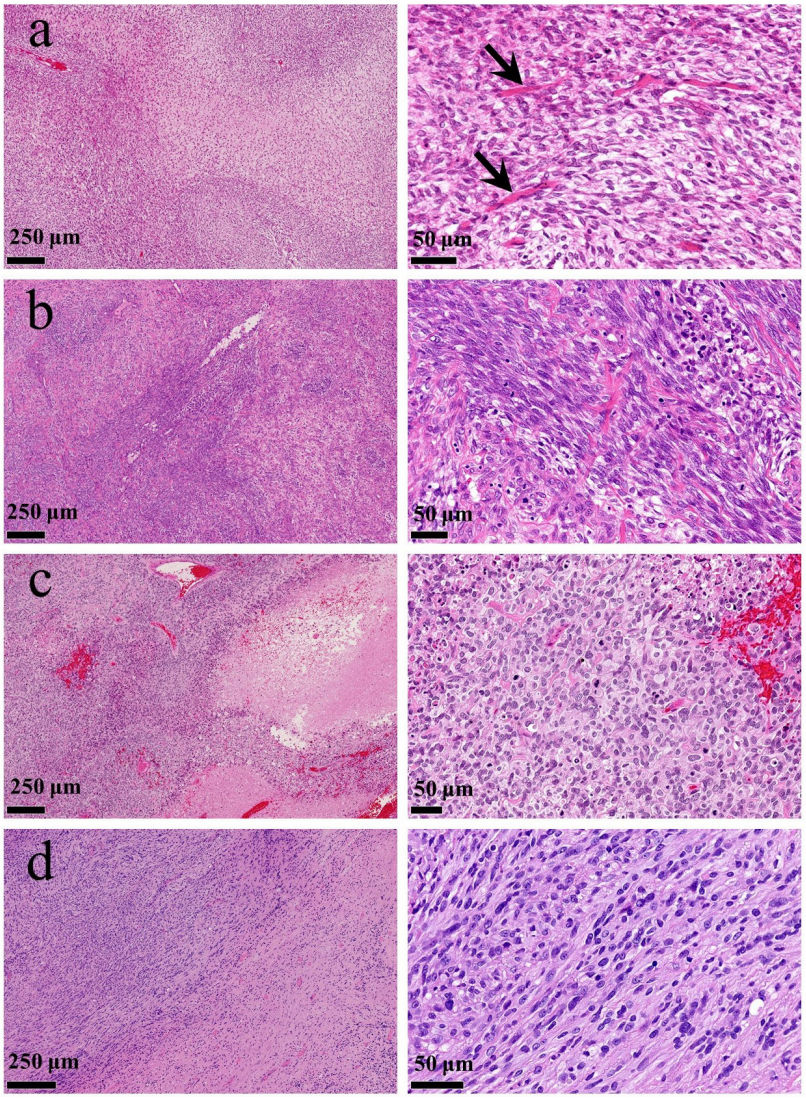

Figure 3

a) Spindle tumor cells show fascicular growth with focal skeletal muscle differentiation (arrows) (hematoxylin and eosin (HE) stain).

b) Atypical spindle cells proliferate in a fascicular pattern (HE stain).

c) The cellular tumor exhibits high-grade nuclear atypia (HE stain).

d) Spindle-shaped tumor cells show fascicular growth (HE stain).

Spindle cell sarcomas with alternating cellularity and brisk mitotic activity, typical of the pathology in MPNST, are present in all cases. No differences are apparent between **a**) and **b**) or **d**) other than the focal skeletal muscle differentiation in **a**). Although **c**) represents a so-called 'anaplastic MPNST', all four cases correspond to high-grade MPNST comprising sarcoma with high cellularity.

Table 1 Sonographic findings of malignant and benign neurogenic tumors, including the present 4 cases of MPNST

	Malignant soft tissue tumors in general	MPNST: 4 cases in the present study	MPNST: cases reported with sonographic findings	Neurofibroma	Schwannoma (=Neurilemoma)
Maximal diameter	≥ 46 mm; >50 mm	210 mm; 97 mm; 119 mm; >144 mm	mean 56 mm (42–110 mm); large (but not described); 50 mm	mean 22 mm (2–49 mm)	≤ 50 mm
Location		thigh; thigh; retroperitoneum; retroperitoneum	thigh; retroperitoneum		
Shape	irregular or lobulated	oval; lobulated; round; irregular	elongated; fusiform; irregular	oval; extensive lobulated; serpentine and partly oval in plexiform tumors	oval > lobulated; peripheral nerve entering and exiting
Margin	ill-defined	well-defined	ill-defined; well-defined; range from well-defined to infiltrating	well-defined; ill-defined	well-defined
Echogenicity	hypo, iso or hyper	hypo	hypo	hypo	hypo
Texture	heterogeneous	heterogeneous	heterogeneous (with necrosis, hemorrhage and/or calcification)	homogeneous; more heterogeneous than schwannomas	homogeneous but heterogenous due to degeneration in 'ancient' (larger) tumors
Vascularity	hyper	hyper	hyper; intrinsic anarchic vascular pattern with spectral waveform; flow within cystic area; stenosis, occlusion, trifurcation and archaic vascular pattern	hypo	hyper
Posterior enhancement	(not described)	not detected	present	present	present
Target sign (hyperechoic central area with hypoechoic periphery)	(not described)	absent	rarely present	present	present; rarely present

Abbreviation: MPNST, malignant peripheral nerve sheath tumor.

though the margins were well-defined, the contours were irregular and textures in the tumors were heterogeneous. Doppler sonography showed hyper-vascularity with internal vessels. MRI showed a mass measuring 160 × 110 mm in the left retroperitoneum that had invaded both the erector spinae muscles and the spinal canal (**Figure 2g, h**). The mass exhibited heterogeneous hypo- to isointensity as compared with abdominal fat or muscle on T1-weighted imaging, and heterogeneous isointensity intermingled by signal hyperintensity suggesting hemorrhagic necrosis on T2-weghted imaging. While sonographic examination depicted the mass as two lesions, MRI showed that these lesions were connected. A biopsy specimen from the mass revealed mitotic figures present at a rate of 15 per 10 high-power fields, and diagnosed as a MPNST (**Figure 3d**).

IV. DISCUSSION

MPNSTs are histologically classified into four subtypes: conventional, malignant triton tumor, glandular, and epithelioid types [3) 6) 15) -17)]. Conventional MPNST is the most common, accounting for 80–85% of MPNSTs. The remaining 15% comprise the other three subtypes with various differentiations. Malignant triton tumor defined as MPNST with rhabdomyoblastic differentiation as seen in Case 1 of the present study accounts for 5% of MPNSTs and exhibits aggressive behavior with poor outcomes as compared with conventional MPNST [18)]. Cases 1 and 2 finally underwent surgical resection. Although the contour was regular or lobular in each tumor, the margins were well-defined on sonography (**Figure 1a-d; Table 1**), which represented nodular lesions macroscopically. Cases 3 and 4 were pathologically diagnosed from the biopsied specimens. Although the contours of Cases 3 and 4 tumors were regular and irregular, respectively,

Table 2 MRI findings of MPNST and representative benign neurogenic tumors

	MPNST	Neurofibroma	Schwannoma (Neurilemoma)
Age	20–50 years	20–30 years	20–40 years
Size	large, >5 cm		
Shape		fusiform (with tapered ends); multilobulated	fusiform (with tapered ends)
Margin	poorly defined; well-defined	well-defined	well-defined
Texture	heterogeneous, including intratumoral cystic areas suggesting hemorrhage or necrosis	homogeneous on T1; heterogeneous on T2	heterogeneous
MRI: T1 / T2	low or intermediate; iso to adjacent muscle (high representing hemorrhage)/ heterogeneous high	low or intermediate; iso to skeletal muscle / heterogeneously high	low or intermediate / heterogeneously high
Enhanced MRI (contrast-enhanced T1)	heterogeneous peripheral enhancement with non-enhancing areas representing cystic changes or necrosis	hyper homogeneous and patchy mild reversed target sign	hyper with or without internal cystic areas
Target sign	absent; rarely present	present (hyperintense ring and hypointense center on T2WI)	present (peripheral high and central low on T2WI)
Split fat sign	absent	present	present
Perilesional edema	present	absent	absent

Abbreviations: MPNST, malignant peripheral nerve sheath tumor; MRI, magnetic resonance imaging; WI, weighted imaging.

the margins were well-defined in both (**Figure 1e-h; Table 1**). However, contrast with the macroscopic pathology could not be performed because the diagnoses were made from of biopsied specimens. The heterogeneous internal texture observed in all four cases (**Figure 1; Table 1**) could have been due to spindle cell sarcomas with alternating cellularity and brisk mitotic activity, typical for the pathology of MPNST (**Figure 3**). No differences were noted between Case 1 and Cases 2 and 4 other than focal skeletal muscle differentiation in Case 1. Although Case 3 was a so-called 'anaplastic MPNST', all four cases corresponded to high-grade MPNST comprising sarcoma with high cellularity. Intermingled anechoic areas in Cases 1 and 3 (**Figure 1a, e**) may have corresponded to necrotic and hemorrhagic areas in malignant triton tumor type and anaplastic MPNST (**Figure 3c**).

When compared with benign soft-tissue tumors, malignant soft-tissue tumors generally exhibit large size, ill-defined margins and hypervascularity on sonography, as described in our previous study [9) 19)]. In contrast, no differences are found concerning echogenicity or internal texture between benign and malignant soft-tissue tumors (**Table 1**). The present four cases suggest that MPNST forms a large, well-defined, heterogeneously hypoechoic mass with hypervascularity. The features of large size and hypervascularity are consistent with those of malignant soft-tissue tumors in general. In contrast, the well-defined margin could serve as a distinct feature of MPNST, differing from the general finding of malignant soft-tissue tumors. Actually, three case reports of MPNST have demonstrated well-defined margins on sonographic imaging [18) 20) 21)]. This supports our hypothesis that MPNST is likely to show well-defined margins on sonography.

The most recent study utilizing sonography in a large group of patients with PNSTs concluded that MPNST shows an ill-defined margin [10)]. That study settled on the strict numerical criteria for evaluations of tumor margin, as follows: well-defined, > 90% of whole margin is well demarcated; and ill-defined, ≤ 90% of the whole margin is well demarcated. However, tumor margins have been evaluated qualitatively by trained sonographers on sonography in most studies, including our own [9) 13) 14)]. Since tracing the whole margin of these mostly large MPNSTs could be difficult within the restricted field of vision on sonography, the criterion of whether over or less than 90% of the tumor margin is well- or poorly demarcated on sonography [10)] may not be practical. Because our criteria for evaluating the tumor margin have been concordant in most previous studies applying non-numerical criteria [22)-25)], the margin for MPNST should be considered well-defined in clinical practice.

Among the current imaging examination modalities,

MRI has been the most advantageous to diagnose soft-tissue tumors, including MPNST, because of its ability to evaluate tumor properties. Representative findings on MRI for MPNST are shown in **Table 2**. MPNST has been reported to exhibit well-defined or partially ill-defined margins on MRI as compared with non-neurogenic malignant soft-tissue tumors [11) 18)]. A large series investigating differential features on MRI between MPNST and neurofibroma identified that both tumors exhibit well-defined margin with no significant differences [7)]. Meanwhile, that study also concluded that two or more among the four features of tumor size, peripheral enhancement, perilesional edema and intratumoral cystic change could augment discrimination of MPNST from neurofibroma. Another study demonstrated that a recent advance in MRI using diffusion-weighted imaging values combined with conventional MRI findings could discriminate MPNST from benign tumors [26)]. However, ill-defined margins were included among the conventional MRI findings suggesting MPNST in that study. Thus, the use of well- or poorly defined margins for the diagnosis of MPNST on MRI has varied between studies. MRI has actually been serving as the most reliable imaging modality to diagnose soft-tissue tumors, including MPNST, because several sequences provide tumor features. However, MRI remains challenging in terms of accessibility due to cost, low procedural throughput, and invasiveness for some patients, such as those with pacemakers. Further, not all institutions can equip themselves with MRI machines.

In contrast, sonography could solve these problems, particularly as an initial imaging examination. When encountering tumors originating from soft tissues on sonography, a large mass with ill-defined margin and hypervascularity on Doppler imaging could be suggestive of malignant tumors in general [9)]. Homogeneous masses with well-defined margins may well be benign tumors, but even if well-defined margins are present, heterogeneous masses may be malignant. Examiners should therefore be cautious in reporting. The probability of MPNST should increase considerably, especially for large, rapidly growing masses with well-defined margins, although the hypoechogenicity, heterogeneous internal texture and hypervascularity seen in MPNST could not be definitively discriminated from the features in benign tumors (**Table 1**) [18)-21)27)-29)].

Basically, half of MPNSTs arise from preexisting neurofibromas in patients with NF1, as in Cases 1, 3 and 4. Development of MPNST should thus always be considered in patients with NF1 [4) 5)]. MPNST can also develop sporadically in otherwise normal tissues [6)]. When a rapidly growing mass exhibits sonographic findings similar to those in the present cases in the soft-tissues of patients, especially those with a history of NF1, MPNST should be considered among the differential diagnoses.

As a limitation of sonographic examinations as compared with MRI in the diagnosis of MPNST, tracing the entire margin of a tumor could be difficult in the restricted field of vision because of the large size of most MPNSTs, as described above. Further, tumor invading bones or bone marrow may not be depicted. MPNSTs arising from areas in the trunk such as the pleural cavity or retroperitoneal cavity might be difficult to observe, depending on conditions such as gas in the body. The internal texture of MPNSTs could be heterogeneous on sonography, while several sequences on MRI can evaluate the detailed context of tumor textures. Contrast-enhanced sonography is better than Doppler sonography for evaluating tumor vascularity, as contrast-enhanced MRI uses gadolinium in addition to several sequences of MRI [30)]. Histopathological differences might thus be partly responsible for the differences in sonographic images of MPNSTs. The possible contribution of histological differences in MPNST subtypes to sonographic image differences remains to be clarified by accumulating more cases of this rare pathology.

V. CONCLUSION

The present study clarified several sonographic findings characteristic of MPNST that are similar to those observed in malignant soft-tissue tumors, such as heterogeneity and hypervascularity. A well-defined margin could represent a point of distinction from malignant soft-tissue tumors in general. Sonography alone may not warrant a definitive diagnosis of MPNST, but seems useful as an initial imaging modality. When a large, hypervascular tumor with features of malignant soft-tissue tumor exhibits a well-defined margin on sonography, MPNST should be considered as a differentiated diagnosis.

Acknowledgements:

This work was supported by a research fund from the Kyorin University Faculty of Health Sciences (Grant Number: R401010001).

Authorship contributions:

MO and NS performed the sonographic examinations and evaluated the imaging findings. TK contributed to the conception and design of the study, and wrote the manuscript. SM created figures. SY, KO and HY provided suggestions during the study. TM performed the sur-

geries in Cases 1 and 2. JS pathologically diagnosed the cases. TW gave comprehensive advice on the study and manuscript. HO revised the manuscript. All authors read and approved the final version of the manuscript.

Conflict of interest:

Maiko Osaka, Tomonori Kishino, Naoko Shimamori, Satsuki Matsushima, Satoko Yamasaki, Kouki Ohtsuka, Hiroki Yasudo, Takeshi Morii, Junji Shibahara, Takashi Watanabe, and Hiroaki Ohnishi declare that they have no conflict of interest.

REFERENCES

1) Lin J, Martel W. Cross-sectional imaging of peripheral nerve sheath tumors: characteristic signs on CT, MR imaging, and sonography. AJR Am J Roentgenol 2001; 176 (1) : 75-82. doi: 10.2214/ajr.176.1.1760075.
2) Durbin AD, Ki DH, He S, et al. Malignant peripheral nerve sheath tumors. Adv Exp Med Biol 2016; 916: 495-530. doi: 10.1007/978-3-319-30654-4_22.
3) Nielsen GP, Chi P. Malignant peripheral nerve sheath tumour. In: WHO Classification of Tumours Editorial Board, editor. WHO Classification of Tumours, 5th ed., Vol.3, Soft Tissue & Bone Tumours, WORLD HEALTH ORGANIZATION; 2020, p.254-7.
4) James AW, Shurell E, Singh A, et al. Malignant peripheral nerve sheath tumor. Surg Oncol Clin N Am 2016; 25 (4) : 789-802. doi: 10.1016/j.soc.2016.05.009.
5) Miettinen MM, Antonescu CR, Fletcher CDM, et al. Histopathologic evaluation of atypical neurofibromatous tumors and their transformation into malignant peripheral nerve sheath tumor in patients with neurofibromatosis 1 - a consensus overview. Hum Pathol 2017; 67: 1-10. doi: 10.1016/j.humpath.2017.05.010.
6) Abdel Razek AAK, Gamaleldin OA, Elsebaie NA. Peripheral nerve sheath tumors of head and neck: imaging-based review of World Health Organization classification. J Comput Assist Tomogr 2020; 44 (6) : 928-40. doi: 10.1097/RCT.0000000000001109.
7) Wasa J, Nishida Y, Tsukushi S, et al. MRI features in the differentiation of malignant peripheral nerve sheath tumors and neurofibromas. AJR Am J Roentgenol 2010; 194 (6) : 1568-74. doi: 10.2214/AJR.09.2724.
8) Koike H, Nishida Y, Ito S, et al. Diffusion-weighted magnetic resonance imaging improves the accuracy of differentiation of benign from malignant peripheral nerve sheath tumors. World Neurosurg 2022; 157: e207-14. doi: 10.1016/j.wneu.2021.09.130.
9) Morii T, Kishino T, Shimamori N, et al. Differential diagnosis between benign and malignant soft tissue tumors utilizing ultrasound parameters. J Med Ultrason (2001) 2018; 45 (1) : 113-9. doi: 10.1007/s10396-017-0796-3.
10) Jin Z, Zhao K, Guo W, et al. Investigation of ultrasound parameters for the differential diagnosis of malignant and benign peripheral nerve sheath tumors. J Ultrasound Med 2022; 41 (12) : 3091-101. doi: 10.1002/jum.16089.
11) Van Herendael BH, Heyman SRG, Vanhoenacker FM, et al. The value of magnetic resonance imaging in the differentiation between malignant peripheral nerve-sheath tumors and non-neurogenic malignant soft-tissue tumors. Skeletal Radiol 2006; 35 (10) : 745-53. doi: 10.1007/s00256-006-0160-y.
12) Giovagnorio F, Andreoli C, De Cicco ML. Color Doppler sonography of focal lesions of the skin and subcutaneous tissue. J Ultrasound Med 1999; 18 (2) : 89-93. doi: 10.7863/jum.1999.18.2.89.
13) Shimamori N, Kishino T, Morii T, et al. Sonographic appearances of liposarcoma: correlations with pathologic subtypes. Ultrasound Med Biol 2019; 45 (9) : 2568-74. doi: 10.1016/j.ultrasmedbio.2019.05.020.
14) Shimamori N, Kishino T, Okabe N, et al. Discrimination of well-differentiated liposarcoma from benign lipoma on sonography: an uncontrolled retrospective study. J Med Ultrason (2001) 2020; 47 (4) : 617-23. doi: 10.1007/s10396-020-01051-5.
15) Otsuka H, Kohashi K, Yoshimoto M, et al. Immunohistochemical evaluation of H3K27 trimethylation in malignant peripheral nerve sheath tumors. Pathol Res Pract 2018; 214 (3) : 417-25. doi: 10.1016/j.prp.2017.12.015.
16) Meyer A, Billings SD. What's new in nerve sheath tumors. Virchows Arch 2020; 476 (1) : 65-80. doi: 10.1007/s00428-019-02671-0.
17) Berner EA, Hung YP, Nielsen GP, et al. Malignant peripheral nerve sheath tumors arising from schwannomas: case series and literature review. APMIS 2021; 129 (8) : 524-32. doi: 10.1111/apm.13139.
18) Kamran SC, Shinagare AB, Howard SA, et al. A-Z of malignant peripheral nerve sheath tumors. Cancer Imaging 2012; 12 (3) : 475-83. doi: 10.1102/1470-7330.2012.0043.
19) Chiou HJ, Chou YH, Chiu SY, et al. Differentiation of benign and malignant superficial soft-tissue masses using grayscale and color Doppler ultrasonography. J Chin Med Assoc 2009; 72 (6) : 307-15. doi: 10.1016/S1726-4901 (09) 70377-6.
20) Chatzistefanou A, Mantatzis M, Deftereos S, et al. Peripheral nerve sheath tumors. Benign or malignant? The role of MRI and ultrasonography in a case report. J Neuroimaging 2014; 24 (3) : 308-10. doi: 10.1111/j.1552-6569.2012.00731.x.
21) Jha A, Gupta P, Wahab S, et al. Role of ultrasonography in detection of renal artery pseudoaneurysm caused by retroperitoneal malignant peripheral nerve sheath tumor in a patient with neurofibromatosis type 1. J Med Ultrason (2001) 2014;

41 (1): 87-91. doi: 10.1007/s10396-013-0467-y.

22) Cheng JW, Tang SF, Yu TY, et al. Sonographic features of soft tissue tumors in the hand and forearm. Chang Gung Med J 2007; 30 (6): 547-54.

23) Chen W, Jia JW, Wang JR. Soft tissue diffuse neurofibromas: sonographic findings. J Ultrasound Med 2007; 26 (4): 513-8. doi: 10.7863/jum.2007.26.4.513.

24) Wang Y, Tang J, Luo Y. Sonographic diagnosis of fibromatosis. J Clin Ultrasound 2008; 36 (6): 330-4. doi: 10.1002/jcu.20483.

25) Gong X, Ying H, Zhang Z, et al. Ultrasonography and magnetic resonance imaging features of kaposiform hemangioendothelioma and tufted angioma. J Dermatol 2019; 46 (10): 835-42. doi: 10.1111/1346-8138.15025.

26) Yun JS, Lee MH, Lee SM, et al. Peripheral nerve sheath tumor: differentiation of malignant from benign tumors with conventional and diffusion-weighted MRI. Eur Radiol 2021; 31 (3): 1548-57. doi: 10.1007/s00330-020-07234-5.

27) Lin J, Jacobson JA, Hayes CW. Sonographic target sign in neurofibromas. J Ultrasound Med 1999; 18 (7): 513-7. doi: 10.7863/jum.1999.18.7.513.

28) Grover DSB, Kundra DR, Grover DH, et al. Imaging diagnosis of plexiform neurofibroma- unravelling the confounding features: a report of two cases. Radiol Case Rep. 2021; 16 (9): 2824-33. doi: 10.1016/j.radcr.2021.06.025.

29) Winter N, Dohrn MF, Wittlinger J, et al. Role of high-resolution ultrasound in detection and monitoring of peripheral nerve tumor burden in neurofibromatosis in children. Childs Nerv Syst 2020; 36 (10): 2427-32. doi: 10.1007/s00381-020-04718-z.

30) Costelloe CM, Amini B, Madewell JE. Risks and benefits of gadolinium-based contrast-enhanced MRI. Semin Ultrasound CT MR 2020; 41 (2): 170-82. doi: 10.1053/j.sult.2019.12.005.